



**HAL**  
open science

## Corpus Callosum deformation analysis in Multiple Sclerosis

Foued Derraz, Antonio Pinti, Bruno Lenne, Laurent Peyrodie, Azzeddine Chikh, Abdelmalik Taleb-Ahmed, Patrick Hautecoeur

► **To cite this version:**

Foued Derraz, Antonio Pinti, Bruno Lenne, Laurent Peyrodie, Azzeddine Chikh, et al.. Corpus Callosum deformation analysis in Multiple Sclerosis. AMSE, 2010, 71 (3-4), pp.1-15. hal-00838381

**HAL Id: hal-00838381**

**<https://hal.science/hal-00838381v1>**

Submitted on 26 Jun 2013

**HAL** is a multi-disciplinary open access archive for the deposit and dissemination of scientific research documents, whether they are published or not. The documents may come from teaching and research institutions in France or abroad, or from public or private research centers.

L'archive ouverte pluridisciplinaire **HAL**, est destinée au dépôt et à la diffusion de documents scientifiques de niveau recherche, publiés ou non, émanant des établissements d'enseignement et de recherche français ou étrangers, des laboratoires publics ou privés.

# Corpus Callosum deformation analysis in Multiple Sclerosis

\*F. Derraz, \*\*A. Pinti, \*B. Lenne, \*L. Peyrodie, \*\*A. Taleb-Ahmed,  
\*\*\*A. Chikh, \*P. Hautecoeur.

\*Groupe hospitalier de l'institut catholique de Lille  
Center hospitalier– 59462 Lomme, France  
({hautecoeur.patrick,lenne.bruno }@ghicl.net,  
foued.derraz@icl-lille.fr, laurent.peyrodie@hei.fr )

\*\*LAMIH, FRE 3046 CNRS, Université de Valenciennes - 59300 Valenciennes, France  
({Taleb, Antonio.Pinti }@ univ-valenciennes.fr).

\*\*\*GBM LAB, Université Abou bekr Belkaid, Tlemcen, 13000, Algeria  
az\_chikh@mail.univ-tlemcen.dz

## Résumé

Dans cet article, nous présentons une méthode de mesure des déformations volumiques du Corps Calleux (CC) consécutives à la Sclérose En Plaques (SEP). Une méthode de segmentation 3 D du volume d'intérêt basée sur les modèles déformables est proposée. Des mesures sont ensuite réalisées sur ce volume à partir d'Imagerie par Résonance Magnétique (IRM) cérébrales. La variabilité de la forme géométrique du CC est quantifiée. Les déformations des deux extrémités ainsi que l'épaisseur du corps calleux ont été retenues pour valider la méthode. Les résultats permettent à l'aide du critère établi d'évaluer le taux de déformation causé par la SEP. Celle ci est testée sur une séquences d'IRM de patients à différentes étapes de poussées de la SEP.

## Mot Clés :

Segmentation, sclérose en plaques, corps calleux, imagerie médicale.

## Abstract

In this paper, we propose a new methodology for analyzing the deformations of the Corpus Callosum (CC) volume associated to Multiple Sclerosis (MS) lesion. We propose an approach for 3D segmentation of the volume of interest based on deformable models method. The measures are carried from the segmented brain volume obtained from MR and the deformation of the geometric shape is quantified. The deformations of the two ends as well as the thickness of the CC were retained to validate the method. The results allow evaluating the rate of deformation of the CC among patients from MRI sequences of patients with different level from handicap using the criterion established in this paper.

## Key words :

Segmentation, multiple sclerosis, corpus callosum, medical imaging.

# 1. Introduction

Multiple sclerosis (MS) is a chronic inflammatory disease of the central nervous system characterized by early axonal damage leading to permanent disability in a substantial number of patients. This chronic neurological disability among young adults develops when a threshold of cumulative axonal loss is reached and central nervous system compensatory resources are exhausted (Ouallet 2001). Despite known clinical patterns (Clarysse 2004), there is considerable individual variation in the way of MS and its clinical characteristics, and newer mathematical prognostic models (Inglese 1999) still do not provide satisfactory answers regarding long-term predictability of clinical disability in patients with MS.

Particularly, it allows improving patient follow-up by specifying the diagnosis, the localization of the lesions and the therapeutic monitoring (Quallet 2004). This prospective approach is essential in the study of MS in order to better understand the evaluation of the invalidating disease. MS is a demyelinating disease of the central nervous system that commonly leads to inflammatory and atrophic pathology, and is often associated with cognitive impairment (Benedict 2007, Quallet 2004, Clarysse 2004, Alisa 1991). MS pathology is primarily expressed as focal lesions in the white matter (WM) of the brain, but the state and progression of the disease is also correlated with cerebral atrophy (Fisher 2008).

Because of its superior contrast, magnetic resonance (MR) imaging is the modality of choice for clinical evaluation of MS. Quantitative analysis of MR images to measure and monitor lesion load and tissue has become invaluable for patient follow-up and evaluation of therapies. In recent studies, a correlation was established between the evolution of the MS lesion and the shape deformation of Corpus Callosum (CC) for the MS patient (Yaldizli, 2010). The deformations observed in the CC could thus give an indication on the evolution of the MS lesion and the evolution or proression of the handicap. The CC has a driving role in the connection between the cortical homologous areas and the communication between the two hemispheres. The CC connects the frontal lobes whereas the posterior lobes connects the occipital lobes. Recent work (Fisher 2008, Figueira 2007) associated to the handicap the deficiency of interhemispheric transfer driving and sensory information for MS patients.

The atrophy of the CC would worsen with the evolution of the disease, with a loss from approximately 2% of Corpus Callosum surface per year. This evolution is independent of the evolutionary form of the disease, but would be correlated with the evolution of the handicap (Mortola 2007).

Few studies compared the atrophy of the CC according to the evolutionary form of the disease. A comparative longitudinal study over five years of patients MS-RR (n=75) and MS-SP (n=53), evaluating an index of the callous atrophy (Corpus Callosum index), suggested to include CC atrophy and its progression during follow-up, more marked among patients reached of MS form (Figueira 2007).

The early presence of Corpus Callosum lesions among CIS patients would even be predictive of their risk of conversion towards a clinically definite MS. Thus, in a recent longitudinal study of nearly 158 MS patients, the patients not filling the MRI diagnosis criteria of Barkhof had a risk multiplied by four to develop a clinically definite MS (relative Risk of 3.8) in the event of lesion at the level of the CC (Jafari 2009). This difficulty is due to the diversity of the of classification methods and to the variable number of sub-areas studied (Figueira 2007).

In this paper, we propose a new methodology for analysing CC shape that provides a deformation for MS patient. The method incorporates both spatial and intensity information to segment multichannel MR images (T1, T2, T1 Gado, T2FLair) without post-processing. Although it utilizes multichannel acquisitions, training data are not required to model the intensity distributions, making the algorithm flexible enough to be applied to data originating from a variety of pulse sequences. A novel scheme has been introduced to use the information fused from different input sequences in an efficient way to help active surface based segmentation process.

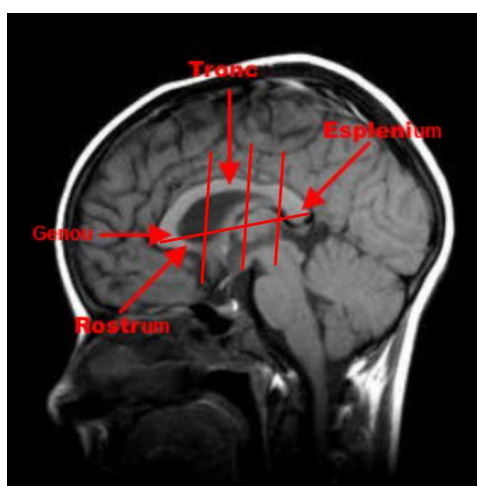


Fig.1: Four segments associated to Corpus Callosum.

The CC shape is divided thereafter into different possible segments. We propose a method to establish geometric relations between the various segments of CC shape. This geometric

method allows us to establish a criterion to help the clinician to identify the deformed cerebral zones of the CC.

## 2. Corpus Callosum extraction method

We propose a methodology of extraction of the CC among patients affected by MS by the method of active surfaces. We organized the CC extraction method according to the flow chart presented on the figure 2.

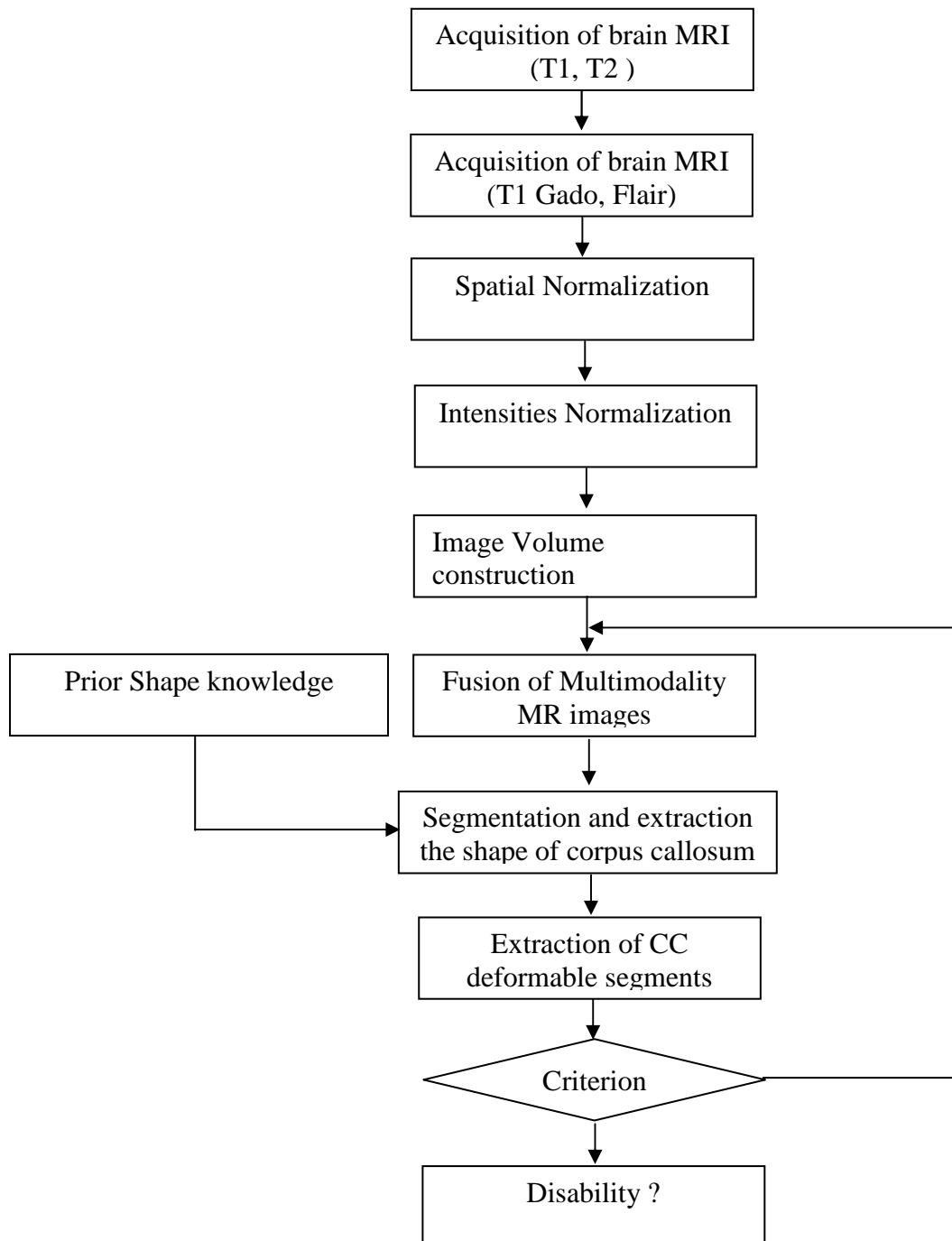


Fig. 2. Flow chart for algorithm to detect deformation of CC shape

In the following sections, we detail the various stages necessary for the extraction of CC and to establish measurements of deformations.

### ***Acquisition protocol of MR Images***

The database of images used within the framework of this article was established at the hospital Saint Philibert (Lomme). It relates to 5 patients and 1 witness, for a total of 6 acquisitions.

The protocols of acquisition of the medical images are: T1 (TE=150, TR=9600, TI=2200), T2 (TE=150, TR=10000, TI=2200), T1Gado (TE=100, TR=9000, TI=2200), FLAIR (TE=120, TR=11000, TI=2200), size of the voxels 0.47\*0.47\*3.3 mm<sup>3</sup>. The images are coded on 12bits/pixel. In spite of its weak resolution in Z and particularly visible artefacts of flow, T2 SENSE OF SMELL is essential to the detection of the lesions of MS, whose contrast is excellent on MRI sequences. It provides segmentation of the lesions however it cannot be used alone for MS. Therefore we also considered the other methods of T2, T1, T1 Gado and T2 FLAIR to improve the segmentation.

### ***Spatial Normalization***

For the needs for the algorithm of extraction, we also need a certification a priori images, i.e. of the prior probability to belong to certain classes (white matter, grey matter, cerebro-spinal liquid) (Mangin,2000) .

### ***Intensity Normalization***

During acquisition, two identical voxels do not have necessarily the same intensity. For that, we used a correction a posteriori of? Skew in the volume of the images to limit these variations during acquisition. The method generally rests on a modeling of the image according to the “real” intensity of the voxel which translates the physical characteristics. Given a voxel of coordinates in the MRI, its intensity is regarded as being connected to the real intensity according to:

$$I = \mathbf{x} + \mathbf{e} \quad (1)$$

where  $\mathbf{e}$  is the bias, generally considered as a function of the coordinates  $(x, y, z)$ , varying slowly in the volume of image, and assumed to be multiplicative according with the intrinsic nature of the subjacent physical phenomena (Magin 2000, Salvado 2006). In our work we corrected skew with a method based on a criterion of an entropic type (Magin 2000, Prima 2001).

### ***Image Fusion***

Lastly, the data resulting from the various methods are fused by Dempster-Shafer rules (Bloch 1997) to obtain a volume of spectral image. Indeed, the MRI can provide various information such the form of intensities of images related to the anatomy by a variety of sequences of

excitations (T1, T2, T1Gado and FLAIR) which can give additional details in order to improve the clinical diagnosis.

The images obtained, starting from the various sequences of excitation, are also called multispectral images. A object volume is composed of various biological elements. A single MRI cannot provide complete information on all the elements to be analyzed. Consequently, the doctors always combine the multispectral information of MRI of the same object to interpret them. The volume of image amalgamated is exploited for the segmentation of the CC (fig. 3).

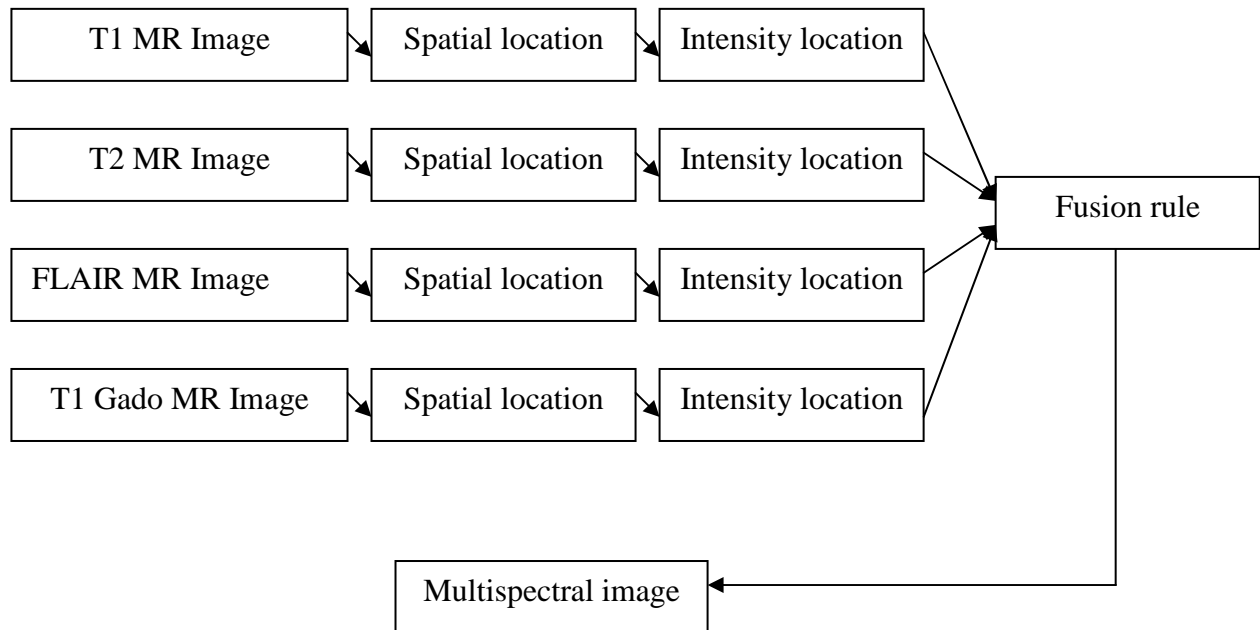


Fig. 3. Flow chart for Fusion of the 4 MRI modalities.

### 3. Corpus Callosum shape extraction method

#### *Segmentation of image volume*

The extraction of the CC shape is very sensitive to the protocols used for MRI acquisition. To extract the shape of CC various approaches are possible (Friston 2006, Akselrod-Ballin 2009). The first approach uses active surface based segmentation method (Horsfield 2007, Akselrod-Ballin 2009). That makes it possible to use local information. However, to segment a volume MRI, an expert makes use of total space information and a priori information of the geometrical form of CC. This method allows us to introduce all terms characterizing space information and the information of the a priori geometric shape to segment the CC. In our case, the equation to be minimized is in the following form:

$$E = \int_{\partial V} k_b(\mathbf{x}, \partial V) da(\mathbf{x}) + \lambda \int_{\partial V} k_{forme\ CC}(\mathbf{x}, \partial V_{ref}) da(\mathbf{x}) + \int_V k_{in\ CC}(\mathbf{x}, V) d\mathbf{x} + \int_V k_{out\ CC}(\mathbf{x}, V) d\mathbf{x} \quad (2)$$

Where  $da(\mathbf{x})$  is the element of volume corresponding to the voxel  $\mathbf{x}$ ,  $\lambda$  is a weighting parameter of the prior shape and  $k_b(\mathbf{x}, \partial V) = 1 / (1 + |\nabla G_\sigma * V|^2)$  is the surfaces descriptor, and  $G_\sigma$  is the Gaussian kernel.

$k_{forme}(\mathbf{x}, \partial V_{ref})$  is the descriptor of the prior shape which will be defined below.  $k_{in}(\mathbf{x}, V)$  and  $k_{out}(\mathbf{x}, V)$  are the descriptors of the inside volume and the outside of active surface delimited by surface  $\partial V$ . They are defined as:

$$k_{inCC}(\mathbf{x}, V) = \log \left( \frac{1}{p(\mathbf{x} \in V_{inCC} | V_I)} \right) \quad (3)$$

$$k_{outCC}(\mathbf{x}, V) = \log \left( \frac{1}{p(\mathbf{x} \in V_{outCC} | V_I)} \right) \quad (4)$$

The criterion to be minimized characterized the area and a priori shape. The evolution equation of the model of active surfaces is obtained by derived Energy function (2):

$$\frac{\partial S}{\partial t} = \left\{ \begin{array}{l} -k_b(\mathbf{x}, \partial V) \kappa - k_{inCC}(\mathbf{x}, V) + k_{outCC}(\mathbf{x}, V) + \lambda k_{formeCC}(\mathbf{x}, \partial V_{ref}) \\ -\lambda \langle \nabla k_{formeCC}(\mathbf{x}, \partial V), \vec{N}_{ref} \rangle + \langle \nabla k_b(\mathbf{x}, \partial V), \vec{N} \rangle \end{array} \right\} \vec{N} \quad (5)$$

where  $\vec{N}$  is the unit vector normal to the surface and  $\vec{N}_{ref}$  the normal vector to prior reference shape.

The prior shape descriptor  $k_{formeCC}(x, \partial V_{ref}) = \frac{1}{2} d^2(\mathbf{x}, \partial V_{ref}) = \min \left( \frac{1}{2} \|\partial V - \partial V_{ref}\|^2 \right)$  calculates the Euclidean distance for maximum similarity between  $\partial V$  and the reference surface  $\partial V_{ref}$ .

Within the levels set framework, the active surfaces model can be formulated by considering that surfaces are represented by  $\omega = \{\mathbf{x} = (x, y, z) \in V_I | \phi(\mathbf{x}) = 0\}$ . The equation of evolution of our model of segmentation is represented implicitly within the level set framework:

$$\begin{aligned} \frac{\partial \phi}{\partial t} = & \left\{ \begin{array}{l} k_b(\mathbf{x}, \partial V) \kappa + k_{inCC}(\mathbf{x}, V) - k_{outCC}(\mathbf{x}, V) \\ + \lambda k_{formeCC}(\mathbf{x}, \partial V_{ref}) \end{array} \right\} \delta(\phi) \\ & - \lambda \left\langle \nabla k_{formeCC}(\mathbf{x}, \partial V), \frac{\nabla \phi_{ref}}{|\nabla \phi_{ref}|} \right\rangle \frac{\nabla \phi}{|\nabla \phi|} + \langle \nabla k_b(\mathbf{x}, \partial V), \nabla \phi \rangle \end{aligned} \quad (6)$$

where  $\delta(\cdot)$  is the Dirac function.



### ***Alignment of shapes***

The surfaces are compared to the reference surface at each iteration; they must each time be aligned according to the minimum of the distance  $d$ . The parameters of alignment are expressed in the following form:

$$\begin{cases} \frac{\partial \mu}{\partial t} = -\lambda \int_V \delta(\phi) d(\mu R\mathbf{x} + T) \nabla d(\mu R\mathbf{x} + T) R\mathbf{x} |\nabla \phi| d\mathbf{x} \\ \mu(0) = \mu_0 \end{cases} \quad (7)$$

$$\begin{cases} \frac{\partial \theta}{\partial t} = -\lambda \mu \int_V \delta(\phi) d(\mu R\mathbf{x} + T) \nabla d(\mu R\mathbf{x} + T) \left( \frac{\partial R}{\partial \theta} x \right) |\nabla \phi| d\mathbf{x} \\ \theta(0) = \theta_0 \end{cases} \quad (8)$$

$$\begin{cases} \frac{\partial T}{\partial t} = -\lambda \int_V d(\mu R\mathbf{x} + T) \nabla d(\mu R\mathbf{x} + T) |\nabla \phi| d\mathbf{x} \\ T(0) = T_0 \end{cases} \quad (9)$$

To have a fast parameter setting we replaced the distance by a standardized distance:

$$d(\phi(\mu R\mathbf{x} + T), \phi_{ref}) = \frac{1}{2} \int_V \left( \begin{matrix} H(\phi(\mu R\mathbf{x} + T)) \\ -H(\phi_{ref}(\mathbf{x})) \end{matrix} \right)^2 \left( \begin{matrix} h(\phi) + \\ h(\phi_{ref}) \end{matrix} \right) d\mathbf{x} \quad (10)$$

Where  $h(\phi)$  is the normalized Heaviside function defined as  $\frac{H(\cdot)}{\int H(\cdot)}$ .

It is this model of retiming which we used in thereafter determining the zones of deformations of the CC. Indeed, we obtain a reference volume which will be compared to the segmented volume.

### ***Segmentation of region of interest of the CC***

We propose to determine the segments of CC by the following method (fig. 4). From the surface of the CC, one determines the maximum distance noted between the two points  $dd_{max}$  from this surface along the sagittal axis which is the principal axis.

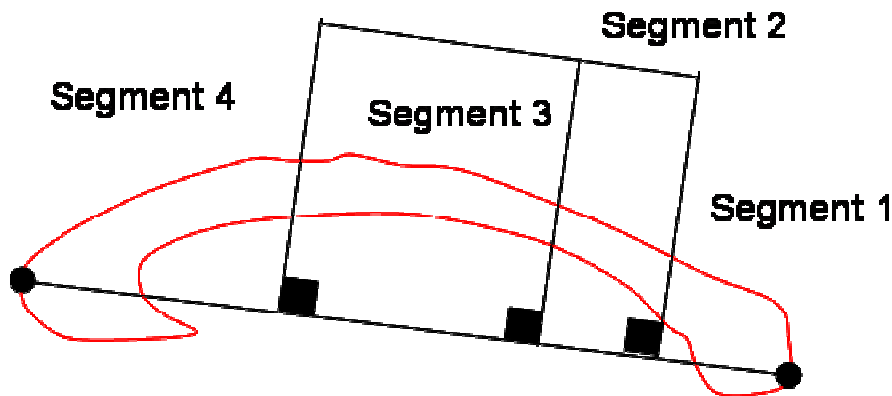


Fig. 4. Partition in 4 segments for the CC.

An orthogonal projection to leave esplenium (fig. 1) 1/10 for the first segment and 1/5 (Trunk) for the second segment and from the 8/10 for the end of the segment nearest to the segment4. The segments are noted respectively by, and. A first deformation can be highlighted by dividing the average height of segment 2 by the surface of this same segment. This cutting in a 3D space gives a volume.

**Mesure of CC deformation by comparing the segmented volumes**

We evaluate the deformations in each zone, the segmented volume  $V_{calc}$  calculated by the active surfaces for CC . A volume ratio is calculated between two values fixed by clinician  $v_{min}$  and  $v_{max}$ .

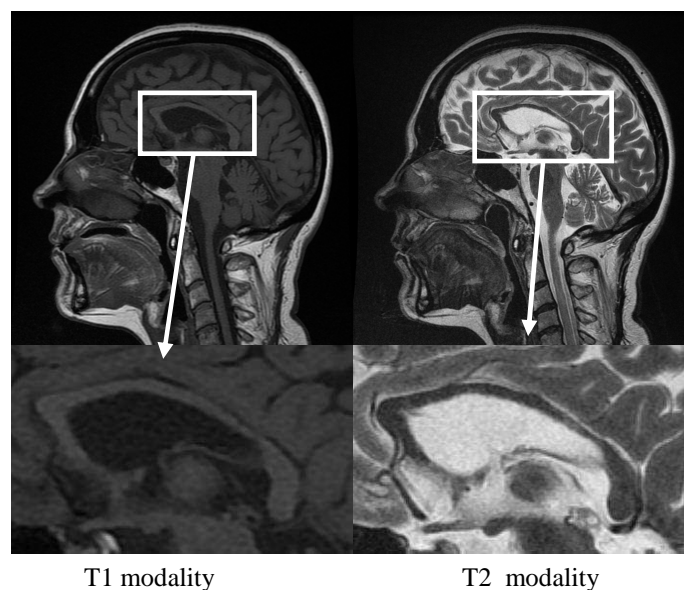
$$v_{min} \leq \frac{V_{calc}}{V_{ref}} \leq v_{max} \quad (11)$$

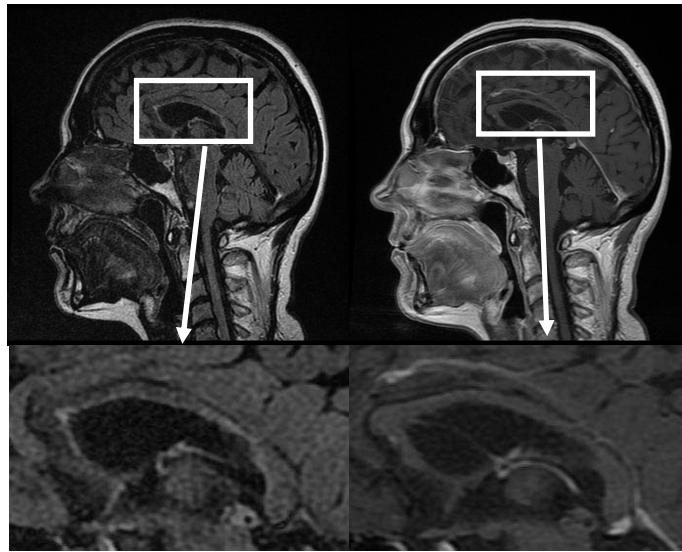
The values  $v_{min}$ ,  $v_{max}$  depend on pathology to study. The deformation is given by:

$$deformation = 1 - \frac{V_{calc}}{V_{ref}} \quad (12)$$

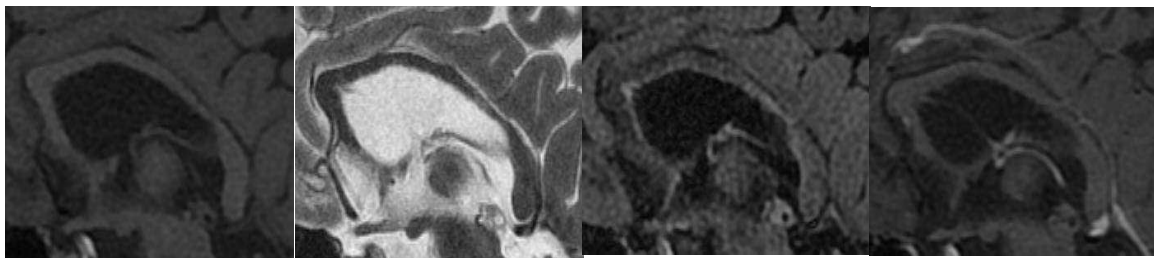
**5. Results**

We tested our method of measurement on five patients suffering from MS with various degrees of handicap and on one healthy case of reference (Table 1). Cognitive tests and an evaluation of EDSS score (scale of quotation of the handicap related to the MS) among patients preceded the examination of the CC by MRI. For each subject, we amalgamated the four imaging methods presented below (Fig 5, Fig 6).





FLAIR T1GADO  
 Fig. 5. Example of MR Images issued for 4 Modalities (T1,T2, Flair, T1Gado).



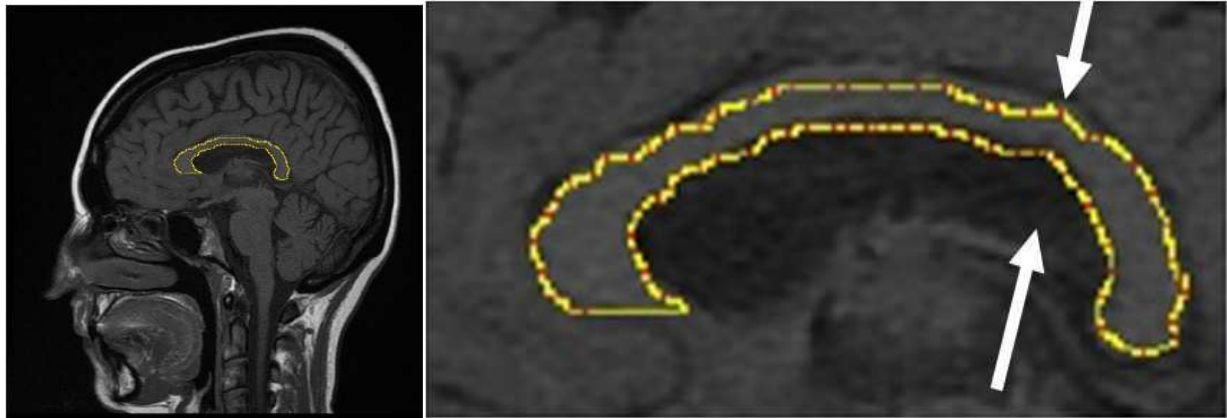
a) ROI of MR images T1, T2, T1Gado, Flair



b) Fused MR images

Fig. 6. Fusion of the MR modalities.

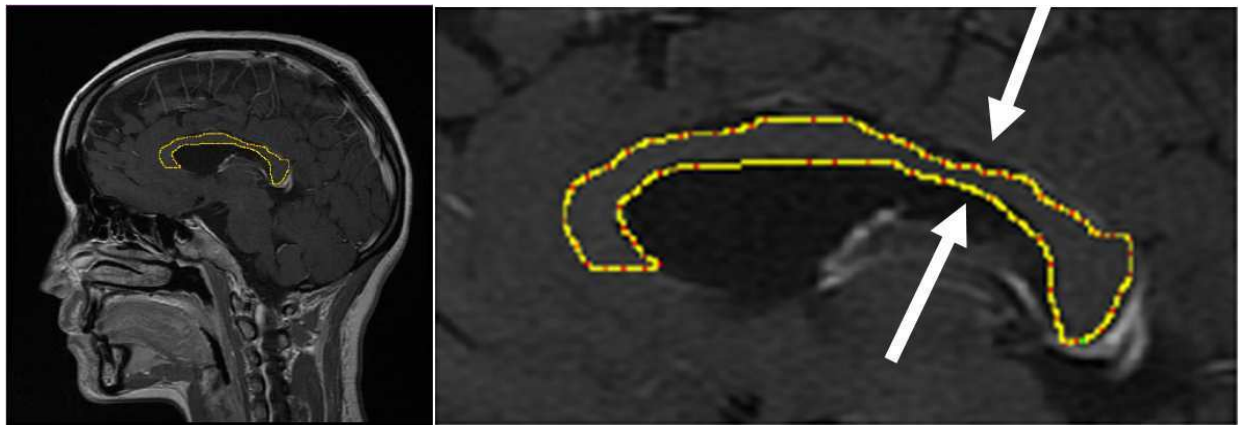
Our model uses the form of reference introduced initially by medical experts. A priori assumption of the shape helps our model of segmentation to find the possible deformations of CC. We present in the figures 7 a) and 8 a) the Sagittal slices of segmented CC.



a) CC segmentation

b) deformation of CC shape.

Fig. 7. Shape deformation of the CC, example 1.



a) CC segmentation

b) deformation of CC shape.

Fig. 8 Shape deformation of the CC, example 2.

The division of CC in four segments makes it possible to isolate the deformed segment (segment 2) and to seek a correlation with information on the handicap caused by MS (score EDSS).

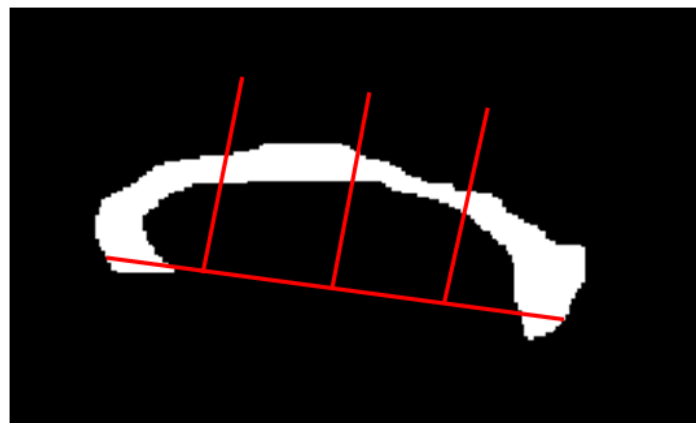


Fig. 9. Measure of deformation of the CC. In white the reference shape and in red the form of the segmented CC.

Thereafter, we represented the deformations of the CC in such manner to have a total view of the consecutive deformations with MS. We represented a frontal view for the knee as well as the possible deformations in space. A view of splenium is given as well as the frontal and longitudinal deformations (fig. 10). The deformations of the CC are given in the sagittal plane with the deformations of the organic areas. A quantitative measurement of this deformation in terms of thickness ration for segment was 2 compared to its surface. In Table 1, we calculated this ratio compared to measurements carried out on organ surfaces. It was observed that the rate of deformation was relatively strong for the subjects with high EDSS score. On the other hand, a low rate of deformation would correspond to a weak EDSS index. This can correlate the rate of deformation calculated starting from a volume of MR image and EDSS scores (index of handicap evaluated by an expert).

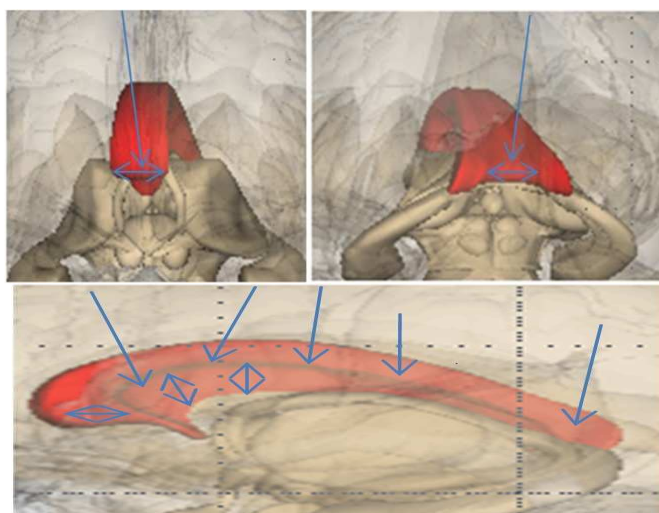


Fig. 10. Visualization of the segmented CC.

N°Patient	Patient old	Sex	MS	EDSS	the disease time in year	Deformation ratio
1	33	F	RR	4	5	14,7%
2	44	F	RR	5	8	17,1%
3	49	F	RR	3.5	16	10,1%
4	28	F	RR	4	1.5	11,1%
5	55	F	RR	4.5	5	15,3%

Table 1. Deformation measure of CC deformation for MS patient

A correlation of 0,802 was found between the values of the EDSS and the rate of deformation, underlining the presence of a positive relation between the rate of incapacity (EDSS) and the deformation of CC. However the small sample (five patients) limits this first encouraging result.

old

## **7. Conclusion**

In this first work, we have proposed a new method of measuring CC deformations for MS patients, this pathology being accompanied very frequently by a CC atrophy. The extraction of the CC data was carried out starting from the segmentation of the volume of multispectral images (T1, T2, T1Gado, T2Flair), with a priori assumption of the shape. In the second time, the division of CC volume in four regions using segments (surface) allows to isolate the area presenting a deformation. A quantitative analysis of the deformations of the various segments was carried out. This deformation was measured by a factor varying from with (for the report of deformation). This deformation was compared with an index evaluating the degree of handicap of patients (EDSS, evaluated by the doctor). Thus, a significant positive correlation was found between the degree of deformation and the level of handicap.

However, a more detailed study is necessary in order to specify this relation between the deformations and the handicap. The fusion of other heterogeneous information in the model of extraction of the deformations of the CC is also necessary to help the doctor in the interpretation and the decision-making concerning the assumption of responsibility of the patient in connection with his handicap.

## **References**

1. J.C. Ouallet and B. Brochet, "Aspects cliniques, physiopathologiques, et thérapeutiques de la sclérose en plaques", EMC - Neurologie, Vol. 1, no. 4, pp. 415-457, 2004.
2. M. Inglese, M. Rovaris, L. Giacomotti, G. Mastronardo, G. Comi and M. Filippi, "Quantitative brain volumetric analysis from patients with multiple sclerosis: a follow-up study" Journal of the Neurological Sciences, vol. 171, no. 1, pp. 8-10, December 1999,
3. P. Clarysse, F. Frouin, M. Garreau, A. Lalande, J. Rousseau, D. Sarrut and C. Vasseur, "Intégration de connaissances et modélisation en imagerie médicale", ITBM-RBM, Vol. 25, no. 3, pp. 139-149, 2004.

4. Alisa D. Gean-Marton, MD L. Gilbert Vezina, MD Keith I. Marton, MD Gary K. Stimac, MD, PhD Robert G. Peyster, MD Juan M. Taveras, MD Kenneth R. Davis, MD, “Abnormal Corpus Callosum: A Sensitive and Specific Indicator of Multiple Sclerosis”, *J. Neuroradiology*, vol. 180, no. 1, pp 215-221, 1991.
5. J. F. Mangin. “Entropy minimization for automatic correction of intensity non uniformity”. *Math. Methods in Biomed. Image Analysis*, pp.162–169, 2000.
6. S. Prima, N. Ayache, Tom Barrick, and Neil Roberts. Maximum Likelihood Estimation of the Bias Field in MR Brain Images: Investigating Different Modelings of the Imaging Process, *MICCAI’01*, vol. 2208 of LNCS, pp. 811–819, 2001.
7. K.J. Friston, J.T. Ashburner, S. Kiebel, T.E. Nichols, and W.D. Penny. *Statistical Parametric Mapping: The Analysis of Functional Brain Images*. Academic Press, 2006.
8. R. Khayati, M. Vafadust, F. Towhidkhah, and M. Nabavi. Fully automatic segmentation of multiple sclerosis lesions in brain mr air images using adaptive mixtures method and markov random field model. *Comput. Biol. Med.*, vol. 38, no.3, pp. 379-390, 2008.
9. O.Salvado, C. Hillenbrand, Zhang Shaoxiang, D.L. Wilson, “Method to correct intensity inhomogeneity in MR images for atherosclerosis characterization”, *IEEE Trans on Medical Imaging*, vol. 25, no.5, pp. 539–552, 2006.
10. A. Akselrod-Ballin, M.Galun, J.M. Gomori, M. Filippi, P. Valsasina, R. Basri, A. Brandt, “Automatic Segmentation and Classification of Multiple Sclerosis in Multichannel MRI”, *IEEE Trans on Biomedical Engineering*, vol.56, no.10, pp. 2461 – 2469, 2009.
11. M.A. Horsfield, R. Bakshi, M. Rovaris, M.A. Rocca, V.S.R Dandamudi, P. Valsasina, E. Judica, F. Lucchini, C.R.G. Guttmann, M.P Sormani, M. Filippi, “Incorporating Domain Knowledge Into the Fuzzy Connectedness Framework: Application to Brain Lesion Volume Estimation in Multiple Sclerosis”, *IEEE Trans on Medical Imaging*, vol.26 , no. 12 , pp.1670 - 1680 , 2007.
12. F. Robichon, P. Bouchard, J.F. Dmonet, M. Habib, “Developmental dyslexia: re-evaluation of the corpus callosum in male adults”, *European Neurology*, vol. 43, no. 4, pp. 233-237, 2000.
13. I. Bloch, H. Maître, ‘Data fusion in 2D and 3D image processing: An overview’, *TSI*, 1997.
14. Ö. Yaldizli, R. Atefy, A. Gass, D. Sturm, S. Glassl, B. Tettenborn and N. Putzki, “Corpus callosum index and long-term disability in multiple sclerosis patients”, *Journal of Neurology*, vol. 257, no. 8, pp. 1256-1264, 2010.

15. J.F. Kurtzke, "Rating neurologic impairment in multiple sclerosis: an expanded disability status scale (EDSS)". *Neurology*; vol. 33, pp. 1444-1452, 1983.
16. M. Gaspari, D. Saletti, C. Scandellari, S. Stecchi, "Refining an Automatic EDSS Scoring Expert System for Routine Clinical Use in Multiple Sclerosis", *IEEE Transc on Information Technology in Biomedicine*, vol. 13, no 4, pp. 501-511, 2009.
17. Dehmeshki, J.; Barker, G.J.; Tofts, P.S., "Classification of disease subgroup and correlation with disease severity using magnetic resonance imaging whole-brain histograms: application to magnetization transfer ratios and multiple sclerosis", *IEEE Transc, on Medical Imaging*, vol. 21, no. 4, pp. 320-331, 2002.
18. Martola, J., Stawiarz, L., Fredrikson, S., Hillert, J., Bergstrom, J., Flodmark, O. , & Kristoffersen Wiberg, M. (2007). Progression of non-age-related callosal brain atrophy in multiple sclerosis: a 9-year longitudinal MRI study representing four decades of disease development. *J Neurol Neurosurg Psychiatry*, 78 (4), 375-380, 2007
19. Figueira, F. F., Santos, V. S., Figueira, G. M. , & Silva, A. C. (2007). Corpus callosum index: a practical method for long-term follow-up in multiple sclerosis. *Arq Neuropsiquiatr*, 65 (4A), 931-935.
20. Jafari, N., Kreft, K. L., Flach, H. Z., Janssens, A. C. , & Hintzen, R. Q. (2009). Callosal lesion predicts future attacks after clinically isolated syndrome. *Neurology*, 73 (22), 1837-1841.
21. R. Benedict and J. Bobholz, "Multiple sclerosis", *Semin. Neurol.* 27 (1) (2007), pp. 78–85.
22. E. Fisher, J.-C. Lee, K. Nakamura and R.A. Rudick, Gray matter atrophy in multiple sclerosis: a longitudinal study, *Ann. Neurol.* 64 (3) (2008), pp. 255–265.
23. Dana Horakova, Michael G. Dwyer, Eva Havrdova, Jennifer L. Cox, Ondrej Dolezal, Niels Bergsland, Brett Rimes, Zdeněk Seidl, Manuela Vaneckova and Robert Zivadinov, "Gray matter atrophy and disability progression in patients with early relapsing–remitting multiple sclerosis: A 5-year longitudinal study", *Journal of the Neurological Sciences*, vol. 282, no. 1-2, pp. 112-119 , July 2009.